



# The value of dual-energy computed tomography in the evaluation of myocarditis

Mecit Kantarcı   
Ümmügülsüm Bayraktutan   
Abdusselam Akbulut   
Onur Taydaş   
Naci Ceviz   
Fadime Güven   
Hayri Oğul   
Sonay Aydın 

## PURPOSE

The inflammation of the heart muscle is referred to as acute myocarditis. Cardiac magnetic resonance imaging (CMR) has become the primary method for a non-invasive assessment of myocardial inflammation. However, there are several drawbacks of CMR. During the last decade, dual energy computed tomography (DECT) has been used in cardiac imaging. The current study aims to assess the efficacy and feasibility of DECT in acute myocarditis and compare the results to CMR.

## METHODS

This prospective study included patients who had myocarditis but no coronary artery pathology. Two observers evaluated the patients for acute myocarditis using DECT and CMR. CMR was performed on 22 patients within 24 hours of DECT, which was administered within 12 hours following the onset of chest pain. Inter-observer agreement was tested with Cohen's Kappa coefficient, and Spearman's correlation was used to examine the possible correlations. A *P* value of <0.050 was accepted as statistically significant.

## RESULTS

The DECT and CMR agreement was significant for transmural diagnoses, excellent for subepicardial and intramyocardial diagnoses, and perfect for nodular and band-like patterns.

## CONCLUSION

The findings of this study showed that the dark areas on the color-coded iodine map created with DECT were strongly correlated with CMR in acute cases of myocarditis. In addition, DECT is a robust imaging method that can also be used in the diagnosis of acute myocarditis. Furthermore, it provides information about coronary arteries faster and more reliably than magnetic resonance imaging without any limitations.

## KEYWORDS

Dual-energy computed tomography, cardiac magnetic resonance imaging, magnetic resonance imaging, myocarditis

From the Department of Radiology (M.K. ✉ akkanrad@hotmail.com, Ü.B., A.A., F.G., H.O.), Atatürk University Faculty of Medicine, Erzurum, Turkey; Department of Radiology (O.T.), Sakarya University Faculty of Medicine, Sakarya, Turkey; Department of Pediatric Cardiology (N.C.), Atatürk University Faculty of Medicine, Erzurum, Turkey; Department of Radiology (S.A.), Erzincan Binali Yıldırım University Faculty of Medicine, Erzincan, Turkey.

Received 23 July 2021; revision requested 19 September 2021; last revision received 13 November 2021; accepted 16 December 2021.



Epub: 27.01.2023

Publication date: 29.03.2023

DOI: 10.5152/dir.2022.21749

The inflammation of the heart muscle is referred to as acute myocarditis. The etiology of this condition is influenced by infections, toxins, hypersensitivity/autoimmune factors, and drugs. Myocarditis can cause a variety of symptoms, including sudden death or cardiogenic shock, recent onset heart failure due to ventricular dysfunction, chest pain, ventricular arrhythmias, and atrial arrhythmias.<sup>1,2</sup>

Electrocardiography (ECG) findings in some cases of focal myopericarditis are indistinguishable from myocardial infarction with ST segment elevation.<sup>3</sup>

The gold standard for diagnosing myocarditis is an endomyocardial biopsy (EMB).<sup>4</sup> The role of an EMB in diagnosing pathologic entities has evolved over time. The Dallas criteria are controversial because many patients who did not meet the Dallas criteria were eventu-

You may cite this article as: Kantarcı M, Bayraktutan Ü, Akbulut A, et al. The value of dual-energy computed tomography in the evaluation of myocarditis. *Diagn Interv Radiol.* 2023;29(2):276-282.

ally diagnosed with myocarditis.<sup>5</sup> Because of the risk of complications and the low sensitivity of histological studies due to the small sampling area, non-invasive diagnostic tests are required.<sup>6</sup> According to one study, increased myocardial delayed enhancement with cardiac magnetic resonance imaging (CMR) correlates well with the presence of an active inflammatory process detected in the histopathology of EMBs.<sup>7</sup> In patients with suspected myocarditis, CMR has become the primary method for a non-invasive assessment of myocardial inflammation.<sup>7-11</sup> Following the introduction of myocardial mapping, new Lake Louise Criteria (nLLC) were recently published, which redefined imaging diagnoses based on the presence of a T1 criterion [presence of late gadolinium enhancement (LGE) or increased T1 mapping or extracellular volume values] and a T2 criterion (hyperintensity in T2 weighted Short tau inversion recovery or increased T2 mapping values). Results revealed that nLLC improved the CMR diagnostic performance for the diagnosis of acute myocarditis, particularly in cases with unusual clinical presentation.<sup>12</sup> However, there are several drawbacks of CMR, such as the long scan time, the fact that it is not universally available, the high cost, claustrophobia, incompatibility with pacemakers, and the incompatibility of prostheses with this technique.<sup>13,14</sup>

Dual-energy computed tomography (DECT) is a developing technology that provides information about the material composition via image acquisition by varying photon energy levels.<sup>15</sup> During the last decade, DECT has been used in cardiac imaging.<sup>16,17</sup> When different energy levels of X-ray spectra penetrate through iodine as a contrast material, it exhibits unique absorption characteristics. As a result, iodine mapping reveals the distribution of iodine in the myocardium,<sup>16</sup> where the dark areas indicate a lack of iodine,

and DECT precisely detects cardiac perfusion defects.<sup>18,19</sup>

The current study aims to assess the efficacy and feasibility of DECT in acute myocarditis and compare the results to CMR.

## Methods

### Study population

The institutional ethics committee approved the study (ATAUNI-KAEK-19-1-13). All participants were enrolled in the study after providing written informed consent, which was obtained from the parents in pediatric cases.

This prospective study began with the recruitment of 41 consecutive patients admitted to our hospital over a 30-month period for acute chest pain mimicking acute coronary syndrome, with high troponin levels but no specific ECG findings indicating typical ischemia.

Exclusion criteria for coronary diseases included the following: (1) a history of cardiac bypass surgery (one patient); (2) a history of coronary stenting (two patients); and (3) the presence of coronary stenosis or occlusion on DECT (two patients). Another five patients were ruled out due to chronic renal failure an unstable hemodynamic state (one patient), and a high heart rate (>80 beats per minute) that made them susceptible to DECT artifacts (three patients). In addition, seven cases (four DECT studies and three CMR studies) with poor image quality and numerous artifacts were eliminated from further consideration. Two patients were ruled out due to claustrophobia. The study group included 22 patients who met the selection criteria (13 males, 9 females; median age, 14 years; range, 1–22 years).

### Study design

Within 12 hours of the onset of chest pain, DECT was used to assess these patients. Following DECT, all patients were evaluated by CMR within a maximum of 24 hours. All patients' creatine kinase (CK), CK-muscle/brain (CKMB), troponin I, ECG, and transthoracic echocardiography (TTE) results were recorded.

To assess the image quality of each coronary segment on DECT, the following five-point scale was used: 5, no motion artifacts; 4, minor artifacts (mild blurring); 3, moderate artifacts (moderate blurring without discontinuity); 2, severe artifacts (doubling or discontinuity along the coronary segments);

and 1, unreadable (vessel structures not differentiable). A score of  $\geq 4$  was considered to indicate acceptable image quality.<sup>20</sup>

### DECT protocol

The DECT examinations were carried out using a 64-slice dual-source multi detector CT scanner (Somatom Definition Flash, Siemens Healthcare, Forchheim, Germany). At a flow rate of 5 mL/s, 70 mL of iopromide (ultravist 370 mg/mL, Bayer Schering Pharma, Berlin, Germany) was injected into the right antecubital vein, followed by 60 mL of saline. The region of interest (ROI) was located in the left ventricle using a bolus tracking technique (CARE-bolus, Siemens Healthcare, Forchheim, Germany). The data collection began at a specific time determined by a single ROI system with a trigger threshold of 200 HU in the left ventricle blood pool. Data collection began 8 s after triggering, with data collected in the arterial phase. The scan mode was a retrospective low-pitch ECG-gated scan with ECG pulsing (a prospective protocol could not be applied to the artifacts during the dual-energy protocol). In the retrospective protocol, ECG dose modulation was used for all patients. For each patient, the CT dose index volume and the dose-length product of the DECT scans were recorded.

During the procedure, the patients were instructed to use the deep-inspiration breath-hold technique, and the scan was performed craniocaudally from the subcarinal level to the diaphragm. For the cardiac cycle, the reconstruction window of the initial axial images was set to 75% (end of diastolic phase) and 45% (end of the systolic phase).

The high- and low-voltage data were reconstructed for the myocardial evaluation using a dual-energy convolution core (D30f) with a temporal resolution of 140 ms and a thickness of 1.5 mm, with 1 mm increments used to optimize the signal/noise ratio. The reconstructed data sets were then tested with a three-material decomposition software analysis platform (Syngo Multimodality Workplace; Siemens, Erlangen, Germany).

### CMR protocol

A 3.0 T magnetic resonance imaging (MRI) device (Magnetom Skyra, Siemens Healthcare, Berlin, Germany) with a 16-channel cardiac coil was used to examine all the patients. All the scans were conducted with the patient in the supine position, and the images were taken during a single breath hold. Gadolinium-enhanced T1-weighted

#### Main points

- Dual energy computed tomography (DECT) is increasingly used for the diagnosis of cardiac pathologies with a reasonable radiation dose, including acute myocarditis. In addition, DECT is strongly correlated with cardiac magnetic resonance imaging in acute cases of myocarditis.
- The combination of a computed tomography coronary angiography and an iodine map with DECT within a single examination can accurately diagnose malignant coronary artery anomalies, coronary artery disease, and acute myocarditis, which can cause symptoms of acute coronary syndrome.

and T2-weighted CMR sequences were obtained by matching with routine short-axis images. After bolus infusion, first-pass perfusion sequences were obtained by injecting 0.1 mmol (i.e., 10–20 mL) of gadoterate dimeglumine (Dotarem; Guerbet, Aulnay-sous-Bois, France) at a rate of 3–4 mL/s, followed by a 30 mL saline flush at the same rate. Next, LGE CMR was performed 10 minutes after the contrast agent was administered intravenously. A two-dimensional phase-sensitive inversion recovery breath-hold sequence was used for LGE imaging at least 10 minutes after the last gadolinium administration. All images were uploaded to the Syngo Multimodality Workplace for review.

### Image analysis

Two radiologists (M.K. and Ü.B., with 13 and 6 years of experience in cardiac CT and MRI, respectively), who were blinded to the clinical data, first independently reviewed the CT images using the 17-segment model according to the American Heart Association classification of the segmentation of the left ventricular myocardium. The main coronary arteries and branches were also evaluated for intraluminal pathologies and anomalies. Before evaluating the myocardium using DECT, on the workstation, the “DE normalize contrast” procedure was applied to standardize the visual evaluation to remove any bias related to inter-observer variability (Figure 1). Arterial phase images were used for the myocardial evaluation. The dark areas on the color-coded iodine map were accepted as pathological fields and recorded for each patient and segment. The two radiologists reached a consensus for the protocol concerning the evaluation of myocarditis when examining the CMR findings of the patients according to the segments at two-day intervals after the DECT evaluation of the combination of coronary CT angiography and iodine map images in a single examination.

A CMR diagnosis of myocarditis was made based on the updated LLC (2018) (Table 1).

The dark areas on the iodine map images on DECT and increased signal intensity areas on the T2-weighted images and LGE in CMR

were noted following a segment-by-segment analysis and visually compared. The number of segments involved, anatomic location (transmural, intramyocardial, subepicardial, subendocardial), and pattern of involvement (nodular, band-like) were also recorded for each segment.

### Statistical analysis

Statistical analyses were performed using SPSS v. 20.0 software (SPSS Inc, Chicago, IL, U.S.A.). Conformity of the data to normal distribution was assessed using the Kolmogorov–Smirnov test. Numerical variables with normal distribution were shown as mean  $\pm$  standard deviation values, variables without normal distribution as median (minimum–maximum) values, and categorical variables as numbers (n) and percentages (%). The sensitivity, specificity, and positive and negative predictive values of observer 1 and observer

2 were calculated according to the segments, location, and pattern obtained from the CMR results. Observers 1 and 2 independently evaluated the CT images for the presence of myocarditis. Cohen’s Kappa coefficient was used to assess the agreement between Observers 1 and 2 regarding the myocarditis diagnosis in terms of the segments, location, and pattern. Accordingly, the degree of agreement was evaluated as slight if the coefficient was 0 to 0.20, fair if it was 0.21 to 0.40, moderate if it was 0.41 to 0.60, substantial if it was 0.61 to 0.80, and almost perfect if it was 0.81 to 1.00.<sup>21</sup> According to the normality assessment of the Kolmogorov–Smirnov test, a Spearman Correlation coefficient was performed for Observer 1, Observer 2, DECT, and CMR data in terms of the total number of segments detected for each patient. A *P* value of <0.005 was accepted as statistically significant.

### Results

An evaluation was made in a total of 22 patients, comprising 13 (59.11%) males and nine (40.90%) females. The mean age of the population and serum concentrations of CK, CKMB, and troponin are shown in detail in Table 2. An infectious episode less than three weeks before admission was reported in 19 patients. For the remaining patients, the primary symptoms were restlessness and acute chest pain. No patient showed signs of cardiac failure or dyspnea. In the ECG, ST-segment elevation was observed in one patient, ST depression was found in three patients, and T-wave inversion was present in five patients. The ECG showed mild tricuspid insufficiency in four patients and left ventricular hypokinesia in five patients. All examinations were completed on time and without any complications. One of the patients had a coronary

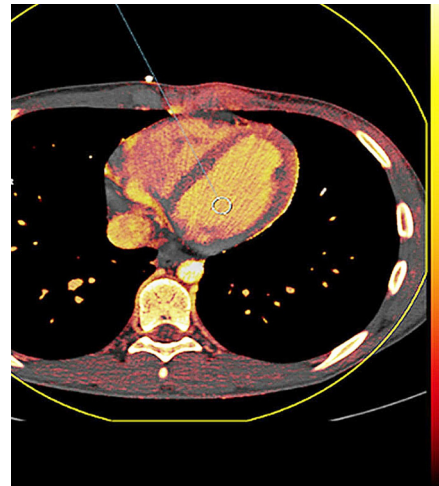


**Figure 1.** The procedure of “DE normalize contrast” (indicated by arrows) in the iodine map on dual energy computed tomography using a dedicated workstation. DE, dual energy.

**Table 2.** Distribution of cardiac enzymes and ages in patients

	Number	Mean $\pm$ SD	Median (min–max)
CK (UI/L)	22	351.18 $\pm$ 75.39	149 (39–3691)
CKMB (UI/L)	22	43.54 $\pm$ 3.81	33 (10–203)
Troponin (ng/mL)	22	8.26 $\pm$ 2.41	0.15 (0.04–85)
Age (years)	22	13.50 $\pm$ 6.62	14 (1–32)

SD, standard deviation; CK, creatine kinase; CKMB, creatine kinase-muscle/brain.

**Table 1.** Updated Lake Louise Criteria (2018)

CMR provides strong evidence for myocardial inflammation with increasing specificity and demonstrates the combination of myocardial edema and inflammatory myocardial injury if both of the following criteria (T1 and T2) are present:

- Regional or global increase of native T2 times or regional or global increase of T2 signal intensity
- Regional or global increase of T1 times, regional or global increase of ECV, or regional non-ischemic LGE signal pattern

Supportive criteria: pericardial effusion, pericardial signal abnormalities, or systolic left ventricle dysfunction

CMR, cardiac magnetic resonance; ECV, extracellular volume; LGE, late gadolinium enhancement.

anomaly. Left anterior descending artery had a course between the aorta and the pulmonary artery. A catheter angiography was not performed since no intraluminal pathology was observed in DECT. All patients were discharged without complications. The patients were checked by laboratory tests (troponin I) and ECG three weeks after the treatment, and no pathology was detected. The cases that previously had pathological findings on TTE also showed improvement. The effective radiation dose of DECT was calculated using a technique proposed by the European

Guidelines on Quality Criteria. The radiation dose parameters for the DECT scans were 315 mGy × cm in the dose-length product, and 7.05 mGy in volume CT dose index.

The dark areas on the iodine map images on DECT and the corresponding increased intensity areas on the T2-weighted scans and LGE in CMR appeared to be nodular or band-like with a subepicardial, intramyocardial, or transmural anatomical location within the left ventricular wall (Figures 2-4). No patient had subendocardial involvement. The dark and normal areas on the iodine map imag-

es on DECT were measured using ROI. The mean value of the dark areas was  $125.67 \pm 40.02$  HU (range, 68–200), while that of the normal areas was  $49.08 \pm 12.90$  HU (range, 30–70).

The involved segments on DECT and CMR are shown in Table 3 according to the evaluation based on the number of segments. Table 4 shows the sensitivity, specificity, and positive and negative predictive values of both observers for the CT diagnosis based on CMR data.

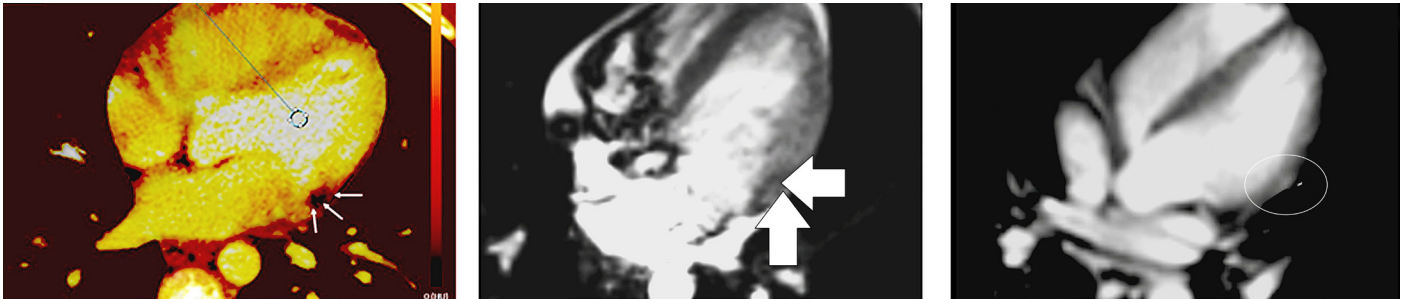


**Figure 2.** Nodular transmural involvement of acute myocarditis. The dark areas on the iodine map on the dual energy computed tomography image (thin arrows), the corresponding edema on the T2-weighted image (thick arrows), and hyperenhancement on the late gadolinium enhancement image (in the circle) in the cardiac magnetic resonance image.

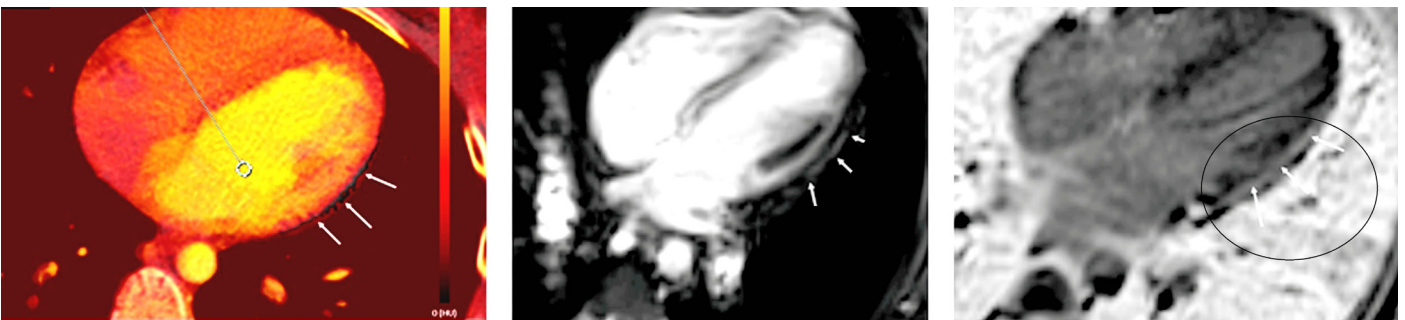


**Figure 3.** Band-like intramyocardial involvement of acute myocarditis. The dark areas on the iodine map on the dual energy computed tomography image (long arrows), the corresponding edema on T2-weighted image (short arrows), and hyperenhancement on the late gadolinium enhancement image (in the circle with arrows) in the cardiac magnetic resonance image. The arrows indicate the band-like intramyocardial involvement of acute myocarditis.

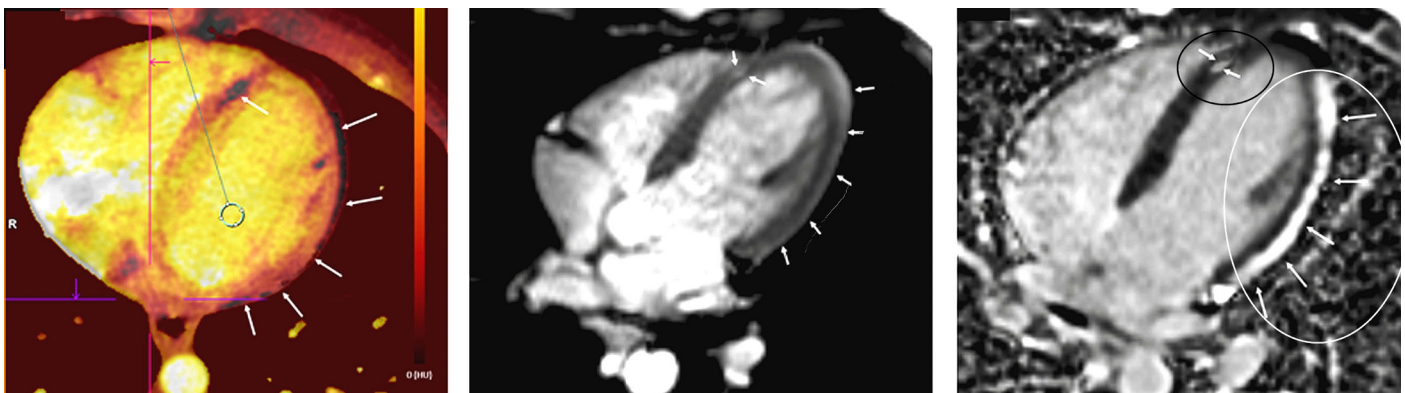


**Figure 4.** Band-like subepicardial involvement of the lateral wall and nodular intramyocardial involvement of the septum of the left ventricle in acute myocarditis. The dark areas on the iodine map on the dual energy computed tomography (DECT) image (single long arrow), the corresponding edema on the T2-weighted image (double short arrow), and hyperenhancement on the late gadolinium enhancement (LGE) image (in the dark circle with arrows) in the cardiac magnetic resonance image (CMR) for nodular intramyocardial involvement of the septum of the left ventricle. The dark areas on the iodine map on the DECT image (multiple long arrows), the corresponding edema on the T2-weighted image (multiple short arrows), and hyperenhancement on the LGE image (in the white circle with arrows) in CMR for band-like subepicardial involvement of the lateral wall.

**Table 3.** Distribution of segments determined by observer 1 and observer 2 on the DECT and consensus MRI findings

Patient	Observer 1 segments on DECT	Observer 2 segments on DECT	Segments on MRI
1	5	5	5
2	4, 5, 6	4, 5, 6	4, 6
3	17, 16, 11, 12, 5, 6	17, 16, 11, 12, 5, 6	17, 16, 11, 12, 5, 6
4	16	16	16
5	6, 12, 4, 10, 2	6, 12, 4, 10, 2	6, 12, 4, 10
6	14, 2	14	14
7	8, 12, 14	8, 12, 14	8, 12, 14
8	14, 8, 9, 3	14, 8, 9	14, 8
9	8, 14, 6	8, 14	8, 14
10	9, 10, 14, 3	9, 10, 14	9, 10, 14
11	2, 3	2, 3	2, 3
12	8, 12	8, 12	8, 12
13	14, 8, 12	14, 8, 12	14, 8, 12
14	12, 14, 1, 2	12, 14	12, 14
15	8, 12	12	12
16	14, 16, 17, 8, 9	14, 16, 17, 8, 9	14, 16, 17
17	12	12	12
18	12, 16	12, 16	12
19	5, 11, 4	5, 11, 4	5, 11
20	11, 12, 16, 8	11, 12, 16	11, 12, 16
21	5, 6, 10, 11	5, 6, 10, 11	5, 6
22	3, 8, 9	3, 8, 9	8, 9

DECT, dual-energy computed tomography; MRI, magnetic resonance imaging.

**Table 4.** Sensitivity, specificity, and positive and negative predictive values of both observers

Observers	Sensitivity (%)	Specificity (%)	Negative predictive value (%)	Positive predictive value (%)
Observer 1	83	87	91	93
Observer 2	89	91	94	96

For observer 1, there was low to moderate agreement between the DECT and CMR findings of segments 2 and 3; substantial agreement for segments 4, 8, 9, and 10; and nearly perfect agreement for segments 5, 6, 11, 12, 14, 16, and 17.

For observer 2, there was low to moderate agreement between the DECT and CMR findings of segment 9; moderate agreement for segment 16; and nearly perfect agreement for segments 5, 8, 11, 12, 14, and 17.

According to the evaluation based on the anatomic location and pattern, the agreement between DECT and CMR was substantial for the diagnosis of transmural involvement, excellent for subepicardial and intramyocardial diagnoses, and almost perfect for nodular and band-like patterns for both observers.

In segments 2, 3 and 16, there was substantial agreement between observer 1 and observer 2, while nearly perfect agreement

was found in the remaining segments (coefficient was 0 to 0.20 fair, 0.21 to 0.40 moderate, 0.41 to 0.60 substantial, 0.61 to 0.80; and almost perfect 0.81 to 1.00) (Table 5).

There was a statistically significant correlation between the total number of segments individually identified on DECT and CMR by observer 1 and observer 2.

**Table 5.** Consensus between observers regarding computed tomography segments

Segment	Kappa	P value
2	0.621	0.002
3	0.621	0.002
4	1.000	<0.001
5	1.000	<0.001
6	0.861	<0.001
8	0.805	<0.001
9	0.831	<0.001
10	1.000	<0.001
11	1.000	<0.001
12	1.000	<0.001
14	1.000	<0.001
16	0.699	0.001
17	1.000	<0.001

**Table 6.** Distribution of correlation between the DECT findings of the observers and the consensus MRI in terms of the total number of segments

	r*	P
Observer 1 DECT - MRI	0.712	<0.001
Observer 2 DECT - MRI	0.769	<0.001
Observer 1 DECT - observer 2 DECT	0.830	<0.001

\*r, correlation coefficient; DECT, dual-energy computed tomography; MRI, magnetic resonance imaging.

The inter-observer agreement was substantial, and the correlation between the total number of segments on DECT identified by both observers was statistically significant.

The correlation was found to be statistically significant in terms of the total number of segments diagnosed between the DECT and CMR findings for both observer 1 and observer 2, as well as in the comparison between the two observers ( $P < 0.001$ ) (Table 6).

## Discussion

In this study, the dark areas on the color-coded iodine map on DECT, which represent pathological myocardial tissue, were compared with the increased intensity areas on the T2-weighted scans and gadolinium enhancement in CMR.

Acute myocarditis is relatively uncommon, and EMB is the gold standard in diagnosis; however, due to its invasiveness and lack of sensitivity, non-invasive techniques have become more popular.<sup>22</sup> Therefore, CMR, with T2-weighted imaging and LGE, has become more widely adopted. Previous studies have shown that CMR correlates with acute inflammation sites histopathologically.<sup>7,9,10</sup> Some studies that use cardiac CT demonstrated that the delayed enhancement areas were similar to those seen on CMR in acute myocarditis.<sup>7,9,10,23</sup>

The DECT technique is used in cardiac imaging to provide information about the coronary artery system and myocardial perfusion with a single contrast-enhanced CT scan obtained within a few seconds using a reasonable radiation dose.<sup>18,24,25</sup> The DECT scans can be obtained with suitable doses similar to single-energy CT.<sup>26</sup> A previous study on cardiac contusion showed the efficiency and feasibility of DECT with a reasonable radiation dose.<sup>27</sup> Moreover, the radiation doses in the current study were lower than those reported in the literature.<sup>28</sup>

A case study of two patients with acute myocarditis showed focal myocardial hypoenhancement areas on an early-phase rou-

tine cardiac CT corresponding to high signals on the T2-weighted MR images and LGE,<sup>29</sup> which were attributed to edema. In another case report, it was found that abnormally delayed iodine enhancement areas on DECT showed an excellent topographic match with CMR.<sup>30</sup>

In the present study, DECT was used to evaluate coronary arteries and myocardial abnormalities. None of the patients had a coronary artery anomaly or pathology. Since malignant coronary artery anomalies and coronary artery disease may lead to similar clinical features to acute myocarditis, it is important to also confirm their presence on DECT. Although DECT is not sufficient to show intraluminal pathologies in distal branches, this study demonstrated its ability to easily show coronary anomalies and intraluminal pathologies in the main branches. In addition, no patient in the current study had a history of coronary artery disease, and the dark areas observed on DECT did not correspond to a coronary artery territory.

Both observers noted that more segments were involved in cardiac DECT than CMR. They were both found to have false positive results. Some of these segments found by observer 1 could be interpreted as beam-hardening artifacts where the heart muscle was thinner. In addition, the literature emphasized that to optimize virtual monoenergetic imaging, the width/length (W/L) setting is crucial.<sup>31,32</sup> Additional research to standardize W/L settings may improve the reliability of DECT in myocarditis imaging.

Some patients in this study had black areas in the late phase on DECT. Early and late enhancements of CMR in myocarditis have been reported in the literature.<sup>33,34</sup> In a comprehensive study by Aquaro et al.<sup>35</sup>, various enhancement patterns in different areas of myocarditis were detected and found to be related to the prognosis. In the current study, although these areas were considered to correspond to early enhancement areas in CMR, the HU values that were measured from these areas were higher than those of the normal myocardium, which creates confusion. Therefore, a histopathological cor-

relation is needed for a clear understanding of this pathophysiology.

There were several limitations to this study, primarily the small patient group. A non-trivial number of initially selected patients were excluded for various reasons, the key subcohort of these patients being those with an inadequate heart rate or suboptimal scan quality. An inadequate heart rate can cause explicit artifacts, which can potentially limit the wider applicability of this technique in this setting. However, this limitation can be overcome by the administration of beta blockers. Larger multicentric and collaborative investigations are required to define the clinical value of DECT and confirm the findings of the current study. Further studies are needed to determine the contrast pattern of the black areas seen in the late phase on DECT. Another limitation was that the distal branches of the coronary arteries could not be assessed due to the technical incompatibility of DECT. Finally, in areas other than the left ventricular free wall, the evaluation was suboptimal due to the beam-hardening artifacts. These limitations could be overcome using advanced technological developments in further DECT studies.

In conclusion, the results of this study showed that the dark areas on the color-coded iodine map on DECT were strongly correlated with CMR in acute cases of myocarditis. The combination of CT coronary angiography and an iodine map with a DECT in a single examination can accurately diagnose malignant coronary artery anomalies, coronary artery disease, and acute myocarditis that can cause symptoms of acute coronary syndrome.

## Conflict of interest disclosure

The authors declared no conflicts of interest.

## References

1. McCarthy RE 3rd, Boehmer JP, Hruban RH, et al. Long-term outcome of fulminant myocarditis as compared with acute (nonfulminant) myocarditis. *N Engl J Med.* 2000;342(10):690-695. [CrossRef]
2. Feldman AM, McNamara D. Myocarditis. *N Engl J Med.* 2000;343(19):1388-1398. [CrossRef]
3. Munguti CM, Akidiva S, Wallace J, Farhoud H. ST segment elevation is not always myocardial infarction: a case of focal myopericarditis. *Case Rep Cardiol.* 2017;2017:3031792. [CrossRef]
4. Aretz HT, Billingham ME, Edwards WD, et al. Myocarditis. A histopathologic definition and classification. *Am J Cardiovasc Pathol.* 1987;1(1):3-14. [CrossRef]

5. Ahmed T, Goyal A. Endomyocardial Biopsy. StatPearls [Internet]. 2021. [\[CrossRef\]](#)
6. Ammirati E, Veronese G, Bottiroli M, et al. Update on acute myocarditis. *Trends Cardiovasc Med.* 2021;31(6):370-379. [\[CrossRef\]](#)
7. Mahrholdt H, Goedecke C, Wagner A, et al. Cardiovascular magnetic resonance assessment of human myocarditis: a comparison to histology and molecular pathology. *Circulation.* 2004;109(10):1250-1258. [\[CrossRef\]](#)
8. Friedrich MG, Sechtem U, Schulz-Menger J, et al. Cardiovascular magnetic resonance in myocarditis: A JACC White Paper. *J Am Coll Cardiol.* 2009;53(17):1475-1487. [\[CrossRef\]](#)
9. Friedrich MG, Strohm O, Schulz-Menger J, Marciniak H, Luft FC, Dietz R. Contrast media-enhanced magnetic resonance imaging visualizes myocardial changes in the course of viral myocarditis. *Circulation.* 1998;97(18):1802-1809. [\[CrossRef\]](#)
10. Laissy JP, Hyafil F, Feldman LJ, et al. Differentiating acute myocardial infarction from myocarditis: diagnostic value of early- and delayed-perfusion cardiac MR imaging. *Radiology.* 2005;237(1):75-82. [\[CrossRef\]](#)
11. Laissy JP, Messin B, Varenne O, et al. MRI of acute myocarditis: a comprehensive approach based on various imaging sequences. *Chest.* 2002;122(5):1638-1648. [\[CrossRef\]](#)
12. Cundari G, Galea N, De Rubeis G, et al. Use of the new Lake Louise Criteria improves CMR detection of atypical forms of acute myocarditis. *Int J Cardiovasc Imaging.* 2021;37(4):1395-1404. [\[CrossRef\]](#)
13. Saeed M, Van TA, Krug R, Hetts SW, Wilson MW. Cardiac MR imaging: current status and future direction. *Cardiovasc Diagn Ther.* 2015;5(4):290-310. [\[CrossRef\]](#)
14. Stokes MB, Nerlekar N, Moir S, Teo KS. The evolving role of cardiac magnetic resonance imaging in the assessment of cardiovascular disease. *Aust Fam Physician.* 2016;45(10):761-764. [\[CrossRef\]](#)
15. Karçaaltıncaba M, Aktaş A. Dual-energy CT revisited with multidetector CT: review of principles and clinical applications. *Diagn Interv Radiol.* 2011;17(3):181-194. [\[CrossRef\]](#)
16. Vliegenthart R, Pelgrim GJ, Ebersberger U, Rowe GW, Oudkerk M, Schoepf UJ. Dual-energy CT of the heart. *AJR Am J Roentgenol.* 2012;199(Suppl 5):S54-S63. [\[CrossRef\]](#)
17. McCollough CH, Leng S, Yu L, Fletcher JG. Dual- and multi-energy ct: principles, technical approaches, and clinical applications. *Radiology.* 2015;276(3):637-653. [\[CrossRef\]](#)
18. Ruzsics B, Lee H, Zwerner PL, Gebregziabher M, Costello P, Schoepf UJ. Dual-energy CT of the heart for diagnosing coronary artery stenosis and myocardial ischemia-initial experience. *Eur Radiol.* 2008;18(11):2414-2424. [\[CrossRef\]](#)
19. Zhao RP, Hao ZR, Song ZJ. Diagnostic value of Flash dual-source CT coronary artery imaging combined with dual-energy myocardial perfusion imaging for coronary heart disease. *Exp Ther Med.* 2014;7(4):865-868. [\[CrossRef\]](#)
20. Bayraktutan U, Kantarci M, Gundogdu F, et al. Efficacy of ivabradin to reduce heart rate prior to coronary CT angiography: comparison with beta-blocker. *Diagn Interv Radiol.* 2012;18(6):537-541. [\[CrossRef\]](#)
21. McHugh ML. Interrater reliability: the kappa statistic. *Biochem Med (Zagreb).* 2012;22(3):276-282. [\[CrossRef\]](#)
22. Felker GM, Thompson RE, Hare JM, et al. Underlying causes and long-term survival in patients with initially unexplained cardiomyopathy. *N Engl J Med.* 2000;342(15):1077-1084. [\[CrossRef\]](#)
23. Dambrin G, Laissy JP, Serfaty JM, Caussin C, Lancelin B, Paul JF. Diagnostic value of ECG-gated multidetector computed tomography in the early phase of suspected acute myocarditis. A preliminary comparative study with cardiac MRI. *Eur Radiol.* 2007;17(2):331-338. [\[CrossRef\]](#)
24. Schwarz F, Ruzsics B, Schoepf UJ, et al. Dual-energy CT of the heart--principles and protocols. *Eur J Radiol.* 2008;68(3):423-433. [\[CrossRef\]](#)
25. Srichai MB, Lim RP, Donnino R, et al. Low-dose, prospective triggered high-pitch spiral coronary computed tomography angiography: comparison with retrospective spiral technique. *Acad Radiol.* 2012;19(5):554-561. [\[CrossRef\]](#)
26. Forghani R, De Man B, Gupta R. Dual-energy computed tomography: physical principles, approaches to scanning, usage, and implementation: part 2. *Neuroimaging Clin N Am.* 2017;27(3):385-400. [\[CrossRef\]](#)
27. Sade R, Kantarci M, Ogul H, et al. The feasibility of dual-energy computed tomography in cardiac contusion imaging for mildest blunt cardiac injury. *J Comput Assist Tomogr.* 2017;41(3):354-359. [\[CrossRef\]](#)
28. Hausleiter J, Meyer T, Hermann F, et al. Estimated radiation dose associated with cardiac CT angiography. *JAMA.* 2009;301(5):500-507. [\[CrossRef\]](#)
29. Brett NJ, Strugnell WE, Slaughter RE. Acute myocarditis demonstrated on CT coronary angiography with MRI correlation. *Circ Cardiovasc Imaging.* 2011;4(3):e5-e6. [\[CrossRef\]](#)
30. Baudry G, Bouleti C, lung B, et al. Diagnosis of acute myocarditis with dual source cardiac tomography. *Int J Cardiol.* 2015;179:256-257. [\[CrossRef\]](#)
31. Caruso D, Parinella AH, Schoepf UJ, et al. Optimization of window settings for standard and advanced virtual monoenergetic imaging in abdominal dual-energy CT angiography. *Abdom Radiol (NY).* 2017;42(3):772-780. [\[CrossRef\]](#)
32. D'Angelo T, Bucher AM, Lenga L, et al. Optimisation of window settings for traditional and noise-optimised virtual monoenergetic imaging in dual-energy computed tomography pulmonary angiography. *Eur Radiol.* 2018;28(4):1393-1401. [\[CrossRef\]](#)
33. Bondarenko O, Beek AM, Hofman MB, et al. Standardizing the definition of hyperenhancement in the quantitative assessment of infarct size and myocardial viability using delayed contrast-enhanced CMR. *J Cardiovasc Magn Reson.* 2005;7(2):481-485. [\[CrossRef\]](#)
34. Bouleti C, Baudry G, lung B, et al. Usefulness of late iodine enhancement on spectral CT in acute myocarditis. *JACC Cardiovasc Imaging.* 2017;10(7):826-827. [\[CrossRef\]](#)
35. Aquaro GD, Perfetti M, Camastra G, et al. Cardiac MR with late gadolinium enhancement in acute myocarditis with preserved systolic function: ITAMY study. *J Am Coll Cardiol.* 2017;70(16):1977-1987. [\[CrossRef\]](#)